



The new International System of Units / *Le nouveau Système international d'unités*

## Silicon spheres for the future realization of the kilogram and the mole



### *Sphères de silicium pour la future réalisation des définitions du kilogramme et de la mole*

Horst Bettin <sup>a,\*</sup>, Kenichi Fujii <sup>b</sup>, Arnold Nicolaus <sup>a</sup>

<sup>a</sup> Physikalisch-Technische Bundesanstalt (PTB), Bundesallee 100, 38116 Braunschweig, Germany

<sup>b</sup> National Metrology Institute of Japan (NMIJ), National Institute of Advanced Industrial Science and Technology (AIST), 1-1-1 Umezono, Tsukuba, Ibaraki 305-8563, Japan

#### ARTICLE INFO

##### Article history:

Available online 17 January 2019

##### Keywords:

XRCD method  
Silicon  
Spheres  
Revised SI  
Planck constant  
Avogadro constant

##### Mots-clés :

Méthode XRCD  
Silicium  
Sphères  
SI révisé  
Constante de Planck  
Constante d'Avogadro

#### ABSTRACT

New definitions of the units for amount of substance – the mole – and for mass – the kilogram – will presumably come into force on the World Metrology Day 2019. In the revised SI, the mole will be defined by a fixed value of the Avogadro constant and the kilogram by a fixed value of the Planck constant. The X-ray-crystal-density (XRCD) method has been used for the determination of these fundamental constants by counting the number of atoms in <sup>28</sup>Si-enriched spheres. Thus, silicon spheres will – after the redefinition – be used to realize the definitions of the mole and the kilogram. This is possible by SI-traceable measurements of lattice parameter, isotopic composition, volume, and surface properties, yielding a relative standard uncertainty below  $2 \cdot 10^{-8}$ . Whereas this high accuracy is only reached with isotopically enriched silicon, it is also planned to use natural silicon spheres on a slightly lower level of accuracy. The future definitions will allow also new realization methods using silicon, in particular for small mass values.

© 2018 Académie des sciences. Published by Elsevier Masson SAS. All rights reserved.

#### R É S U M É

De nouvelles définitions des unités de quantité de matière (la mole) et de masse (le kilogramme) entreront vraisemblablement en vigueur lors de la Journée mondiale de la métrologie de 2019. Dans le Système international révisé, la mole sera définie par une valeur fixe de la constante d'Avogadro et le kilogramme par une valeur fixe de la constante de Planck. La méthode de mesure de densité par cristallographie aux rayons X (XRCD – *X-ray crystal density*) a été utilisée pour déterminer ces constantes fondamentales par comptage du nombre d'atomes dans des sphères de silicium enrichi en silicium 28. Après la redefinition, les définitions de la mole et du kilogramme seront ainsi réalisées à l'aide de sphères de silicium. Ceci est possible en effectuant des mesures des paramètres de réseau, de la composition isotopique, du volume et des propriétés de surface traçables au SI. On obtient alors une incertitude-type relative inférieure à  $2 \cdot 10^{-8}$ . Alors qu'une telle précision ne peut être atteinte qu'avec du silicium enrichi isotopiquement, il est également prévu

\* Corresponding author.

E-mail address: [Horst.Bettin@PTB.DE](mailto:Horst.Bettin@PTB.DE) (H. Bettin).

d'utiliser des sphères de silicium naturel avec un niveau de précision légèrement inférieur. Les futures définitions permettront également de mettre en oeuvre de nouvelles méthodes de réalisation faisant appel au silicium, en particulier pour de faibles valeurs de masses.

© 2018 Académie des sciences. Published by Elsevier Masson SAS. All rights reserved.

## 1. Introduction

In the International System of Units (the SI), the kilogram (kg) has been the last SI base unit still defined by a material artefact. Although this artefact, referred to as the International Prototype of the Kilogram (IPK), has been used since 1889 as the definition of the kilogram, its mass stability was estimated to be about 50  $\mu\text{g}$  because of contamination and damage at its surface. To overcome the limitation in the reproducibility of the kilogram, it was therefore recommended to replace the definition with a fundamental constant of nature.

In the SI revised in 2018, the kilogram is defined by the Planck constant,  $h$ , and the mole (mol) by the Avogadro constant,  $N_A$ . Though the two constants are independently used to redefine the two SI base units, they are closely and rigorously related with each other through other fundamental constants. This is the reason why the method used for measuring the Avogadro constant can be used to realize the revised definition of the kilogram. Comprehensive summaries on the definition and realization of mole and kilogram are included in [1–3]. In this article, we discuss more details on the XRCD method used for realizing the mole and the kilogram.

In the 1960s, Bonse and Hart [4] invented an innovative principle that uses an X-ray interferometer to determine the lattice plane spacing,  $d_{220}$ , of a silicon crystal based on interferometry in the optical wavelength region. Thus, an evaluation of the X-ray wavelength and measurement of the corresponding diffraction angle are not necessary (see section 4).

With the precision polishing technique for manufacturing 1 kg Si spheres [5], it became possible to determine the volume of an Si sample by measurements of its diameter (see section 5).

The accurate determination of the isotopic composition of silicon had proved to be very difficult, since the amounts of the three naturally-occurring Si isotopes could not be measured accurately enough. To overcome this bottleneck in the determination of  $N_A$  and in the future realization of mole and kilogram, isotope enrichment of Si was implemented by the International Avogadro Coordination (IAC) project [6], resulting in a crystal highly enriched in  $^{28}\text{Si}$ . A new concept of applying isotope dilution mass spectrometry to  $^{28}\text{Si}$ -enriched crystals was developed by Rienitz et al. [7]. This method reduced the standard uncertainty in measuring the molar mass,  $M$ , to a few parts in  $10^9$  (see section 6). The relative standard uncertainty in  $N_A$  thus achieved is  $1.7 \cdot 10^{-8}$  [8].

In the revised SI, the mole is defined by  $N_A$ , being independent from the definition of the kilogram. This allows direct measurements of the amount of substance by atom counting (see section 3).

As the surface of a 1 kg silicon sphere is typically covered with thin surface layers with a total thickness of about 1 nm to 2 nm and a total mass of about 100  $\mu\text{g}$ , evaluation of the surface layers is indispensable. Measurements by spectroscopic ellipsometry (SE), X-ray reflectometry (XRR), X-ray photoelectron spectroscopy (XPS), and X-ray fluorescence (XRF) spectrometry are therefore performed for evaluating their thicknesses and masses (see section 7).

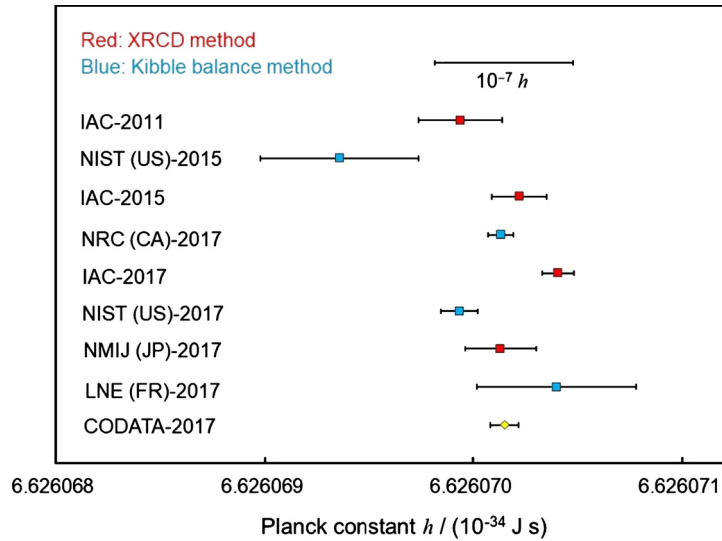
The influence of point defects in silicon crystals on their masses is also not negligible. For example, carbon behaves as substitutional atom; it reduces the lattice spacing of silicon crystals and the unit cell mass. Oxygen is incorporated as interstitial atom; it increases the lattice spacings of silicon crystals and the unit cell mass. Influence of vacancies must be also evaluated. Influence of these point defects on the crystal mass is given in section 8.

Fig. 1 shows the final data selected by the CODATA Task Group on Fundamental Constants, which were used to determine the fixed numerical value of the Planck constant to be used in the revised SI [9,10]. A total of eight data were selected in the CODATA 2017 special adjustment: four (red) were from the XRCD method using  $^{28}\text{Si}$ -enriched silicon crystals and the other four (blue) were from the Kibble balance method. As can be seen from the figure, the uncertainties reported from the two independent methods are almost equivalent, meaning that both methods can be used for realizing the kilogram at the highest level of accuracy.

Considering the statistical consistency of the data, a proposal for the revision of the SI has been set for the 26th General Conference on Weights and Measures (CGPM). The revised SI will come into force on the World Metrology Day (May 20th, 2019).

## 2. Principle of atom counting

Using the combined X-ray and optical interferometry (XROI), the lattice plane spacing,  $d_{220}$ , of silicon can be measured traceable to the SI length unit, the meter (see section 4). Fig. 2 shows the unit cell of silicon – a cube with edge length,  $a$ , which contains eight atoms on average, meaning that the atom at the corner is shared by 8 unit cells and that on the face is shared by 2 unit cells. Considering the geometry of the cubic crystal, the lattice parameter,  $a$ , is determined from the measured value of the lattice plane spacing as  $a = 8^{1/2}d_{220}$ . If the volume,  $V$ , of a macroscopic silicon crystal is measured, the number of atoms,  $N$ , in the crystal is given by



**Fig. 1.** The result of the CODATA 2017 special adjustment [9,10]. Experimental values from the XRCD method using  $^{28}\text{Si}$ -enriched crystals (red) and from the Kibble balance method (blue) are plotted. Their bars express the experimental standard uncertainties. To reach statistical consistency, all the experimental uncertainties were expanded by a factor of 1.7 in deducing the weighted mean value of the Planck constant  $h$  (yellow).

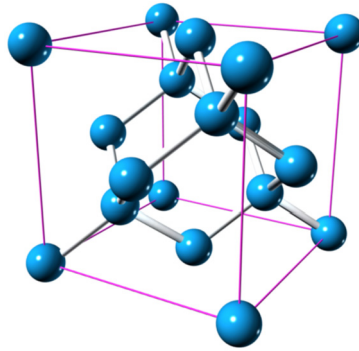


**Fig. 2.** Unit cell of the silicon cubic crystal, with edge lengths equal to the lattice parameter  $a$ .

$$N = \frac{8V}{a^3} \quad (1)$$

where it is assumed that atoms only occupy lattice sites, and that all lattice sites are occupied by silicon atoms (for corrections, see section 8). Consequently, the amount of substance,  $n$ , is expressed as follows:

$$n = \frac{N}{N_A} = \frac{8V}{a^3 N_A} \quad (2)$$

It shall be noted that in the current SI (before the redefinition),  $N_A$  must be measured in conformity with the definition of the kilogram, but in the revised SI, the numerical value of  $N_A$  will be fixed to define the mole. This means that the mole is directly realized by the XRCD method using Eq. (2).

In the XRCD method, a sphere having a mass of approximately 1 kg is normally used, and its volume,  $V$ , is calculated from the measured mean diameter,  $D$  (see section 5). Since silicon crystals are usually covered with thin surface layers having a total thickness of about 1 nm to 2 nm, the measured “apparent” diameter has to be corrected to determine the “core” volume of the sphere without the surface layers (see section 5.5). The core volume is hereinafter referred to as  $V_{\text{core}}$ , and simply deduced from mean core diameter,  $D_{\text{core}}$ , as  $V_{\text{core}} = (\pi/6)D_{\text{core}}^3$ .

### 3. Realization of the mass unit in the revised SI

From the rigorous relations between the fundamental physical constants [11], the rest mass of an electron is expressed as

$$m_e = \frac{2hR_\infty}{c\alpha^2} \quad (3)$$

where  $R_\infty$  is the Rydberg constant,  $c$  is the speed of light in vacuum, and  $\alpha$  is the fine-structure constant. On the right-hand side of Eq. (3), the constants  $R_\infty$  and  $\alpha$  are known with very small uncertainties ( $c$  is already fixed in the definition of the meter in 1983), thus  $R_\infty/(c\alpha^2)$  is known with a relative standard uncertainty of as small as  $4.5 \cdot 10^{-10}$  [12].

Since natural silicon consists of three stable isotopes,  $^{28}\text{Si}$ ,  $^{29}\text{Si}$ , and  $^{30}\text{Si}$ , the isotopic composition, i.e. the amount-of-substance fraction,  $x(^i\text{Si})$ , of each isotope  $^i\text{Si}$  in the crystal must be measured (see section 6) to determine the mean atomic mass of silicon in the crystal. Considering that the mass of each isotope  $^i\text{Si}$  can be expressed as

$$m(^i\text{Si}) = m_e A_r(^i\text{Si})/A_r(e) \quad (4)$$

where  $A_r(^i\text{Si})$  is the relative atomic mass of each isotope  $^i\text{Si}$  and  $A_r(e)$  is the relative atomic mass of electron, the mean atomic mass of silicon is given by

$$m(\text{Si}) = m_e \sum_i x(^i\text{Si}) A_r(^i\text{Si})/A_r(e) \quad (5)$$

with  $\sum_i x(^i\text{Si}) = 1$ . As the values of  $A_r(^{28}\text{Si})$  and  $A_r(e)$  are already known with relative standard uncertainties of  $1.6 \cdot 10^{-11}$  and  $2.7 \cdot 10^{-11}$ , respectively [12], it is possible to determine the mean atomic mass of  $^{28}\text{Si}$ -enriched silicon with a small uncertainty from measurements of  $x(^i\text{Si})$ .

As given in [11], one of the other routes to determine the atomic mass is to directly measure the ratio  $h/m$  by atom interferometry. A new experiment [13] reported that  $h/m(\text{Cs})$  was measured with a relative standard uncertainty of  $4.0 \cdot 10^{-10}$ , suggesting that the atomic mass of  $^i\text{Si}$  can be deduced as  $h[m(\text{Cs})/h]A_r(^i\text{Si})/A_r(\text{Cs})$  with an even smaller uncertainty in the revised SI.

Using Eq. (5), the core mass of a silicon sphere is therefore given by

$$m_{\text{core}} = m(\text{Si})N = 8m(\text{Si})V_{\text{core}}/a^3 \quad (6)$$

Adding the mass of the surface layers,  $m_{\text{SL}}$  (see section 7), correcting for the influence of point defects (i.e. impurities and self-point defects in the crystal) on the core mass,  $m_{\text{deficit}}$  (see section 8), and combining Eqs. (3) to (6), the mass of a silicon sphere is expressed as follows:

$$m_{\text{sphere}} = \frac{2hR_\infty}{c\alpha^2} \frac{\sum_{i=28}^{30} x(^i\text{Si})A_r(^i\text{Si})}{A_r(e)} \frac{8V_{\text{core}}}{a^3} - m_{\text{deficit}} + m_{\text{SL}} \quad (7)$$

In this equation,  $2hR_\infty/(c\alpha^2)$  is the rest mass of the electron,  $\sum_i x(^i\text{Si})A_r(^i\text{Si})/A_r(e)$  the mean mass ratio of silicon to the electron,  $8V_{\text{core}}/a^3$  the number of silicon atoms in the core. Thus, the mass of the whole sphere is characterized completely and can be used to disseminate the unit for mass.

In the current SI (before the redefinition), the molar mass of  $^{12}\text{C}$ ,  $M(^{12}\text{C})$ , has been exactly 12 g/mol by definition. In the revised SI, as the values of  $h$  and  $N_A$  are fixed,  $M(^{12}\text{C})$  is no more a fixed value. Instead, it is a measurand with an uncertainty and is given by  $M(^{12}\text{C}) = N_A m(^{12}\text{C})$ , where  $m(^{12}\text{C})$  is the atomic mass of  $^{12}\text{C}$ . Using the relationship in the mass ratios  $m(^{12}\text{C})/m_e = A_r(^{12}\text{C})/A_r(e) = 12/A_r(e)$ , the molar mass of  $^{12}\text{C}$  in the revised SI is expressed as

$$M(^{12}\text{C}) = \frac{2N_A h R_\infty m(^{12}\text{C})/m_e}{c\alpha^2} = \frac{2N_A h R_\infty A_r(^{12}\text{C})/A_r(e)}{c\alpha^2} = \frac{24N_A h R_\infty}{c\alpha^2 A_r(e)} \quad (8)$$

Similarly, in the current SI (before the redefinition), the molar mass of any nuclide  $X$  is given by  $M(X) = M_u A_r(X)$ , where the molar mass constant,  $M_u$ , has been exactly 0.001 kg/mol. In the revised SI, it is a measurand with an uncertainty and is given by

$$M_u = \frac{2N_A h R_\infty}{c\alpha^2 A_r(e)} = M(^{12}\text{C})/12 \quad (9)$$

The mass of any nuclide  $X$  is expressed as  $m(X) = m_u A_r(X)$ , where  $m_u$  is the unified atomic mass constant defined by  $m_u = m(^{12}\text{C})/12$ . Its relative standard uncertainty is  $1.0 \cdot 10^{-8}$  in the current SI (before the redefinition) [10]. In the revised SI, it is deduced as follows:

$$m_u = \frac{2hR_\infty}{c\alpha^2 A_r(e)} = m(^{12}\text{C})/12 \quad (10)$$

At the time of the adoption of the revised SI, the values of  $M(^{12}\text{C})$  and  $M_u$  are 12 g/mol and 0.001 kg/mol, respectively, within the common relative standard uncertainty of  $4.5 \cdot 10^{-10}$  [10].

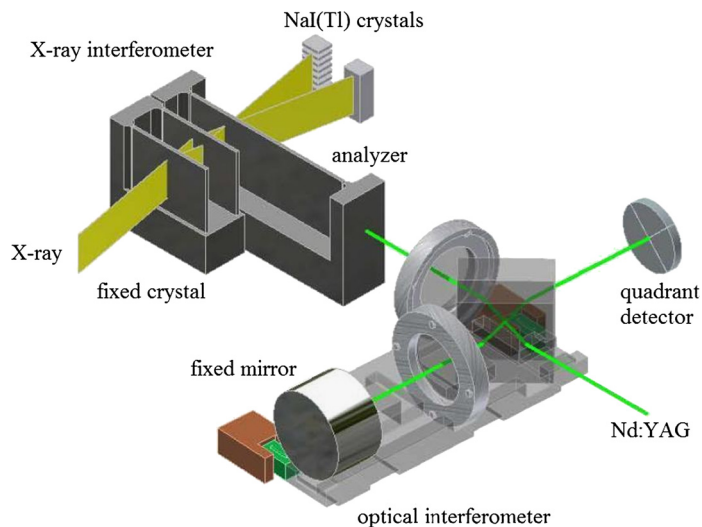


Fig. 3. Schematic drawing of the lattice parameter measurement at INRiM [3].

#### 4. Lattice parameter determination

The unit cell volume  $a^3$  is obtained from the lattice parameter  $a$  of the silicon crystal. For this lattice spacing measurement interferometric technologies with X-ray and optical waves are used.

A typical setup is shown in Fig. 3 [3]. The X-ray interferometer consists of three lamellas, cut out of the Si crystal, oriented in direction of the  $\{220\}$  planes. The X-ray source is of 17-keV Mo  $K\alpha$  type. The first, the “splitter” lamella splits the X-ray into two coherent beams, in the second lamella, the “mirror”, the two beams are reflected and finally recombined in the third, the “analyzer” lamella. This analyzer is in the same distance from the mirror as the splitter lamella from the mirror, so that here the X-rays interfere. If the analyzer is now moved transverse to the beam, it shows a periodic intensity variation with the period of the diffracting-plane spacing. This is detected by NaI (Tl) scintillator crystals and a multi-anode photomultiplier. For the measurement of the movement of the analyzer, an optical interferometer is directed onto the frontal face of the analyzer crystal, so that the lattice spacing or the period of the X-ray fringes, respectively, is measured in units of optical fringes, traced back to a wavelength standard (e.g.  $^{127}\text{I}_2$  stabilized laser at 633 nm or Nd-YAG laser at 532 nm). To overcome the influence of the refractive index of air, the whole instrument is situated in a vacuum chamber.

The lattice parameter of the  $\{220\}$  planes is derived from  $nd_{220} = m\lambda/2$ , herein is  $d_{220}$  the spacing of the  $\{220\}$  lattice planes and  $n$  the number of X-ray fringes that are counted if  $m$  optical fringes with the period of  $\lambda/2$  were measured while the lamella was moved. To increase the measurement speed, only the fractional part of the X-ray fringes is measured at estimated positions of integer values of  $m$ . If  $m$  is increased in an exponential sequence, the measurement time is optimized and the accuracy of the ratio  $\lambda/2:d_{220}$  increases with each step. To eliminate a possible drift between the measurements of the X-ray and the optical interferometer, the analyzer is moved back and forth repeatedly along each of the exponential steps of displacement. As the analyzer lamella is separated from the crystal with the interferometer lamellas, the adjustment is sophisticated and requires exact positioning. Vibrations and imprecise orientation prevent the emergence of any signal. For smallest uncertainties in measuring the lattice parameter, longer displacements of the analyzer are advantageous. At INRiM, a system for position control and alignment of the interferometer crystals was implemented so that the analyzer can be moved up to 50 mm [14]. An optical interferometer with polarization encoding and phase modulation is used to monitor the displacement with picometer accuracy and the rotation in pitch and yaw with nanoradian resolution. For rotation detection, the optical interference pattern is evaluated at four points, so that rotation can be deduced from the differences of their axial displacements. The signals are feedback to a servo loop so that exact positioning and alignment of the X-ray interferometer is assured.

For the determination of the masses of the two spheres worked out of one  $^{28}\text{Si}$ -enriched crystal, the mean lattice parameter of this crystal is to be determined. Contaminants in the silicon can slightly warp the crystal lattice, and due to the mechanisms of the crystal growth, a contamination gradient along the crystal axis is possible. The X-ray interferometer is cut out of the crystal in an axial position between the two spheres, so that it can be assumed that the lattice parameter measured meets in average that of the two spheres. Except for carbon, oxygen and nitrogen, the contents of which are measured, the contaminant concentrations are significantly less than one atom in  $10^9$  Si atoms. Apart from the strain due to different contaminants, it must be ensured that the lattice parameter measured with the X-ray interferometer is measured for the same crystal conditions as for the spheres. This might be influenced by stress and strain due to surface relaxation and reconstruction, and the influence of surface layers. For the big spheres about 94 mm in diameter, a change in the lattice parameter due to surface layers is scarcely to be expected. For the X-ray interferometer lamellas with a thickness of about 1 mm, calculations of the density function by the University of Cagliari (Italy) for an  $\text{SiO}_2$  surface layer indicated a surface

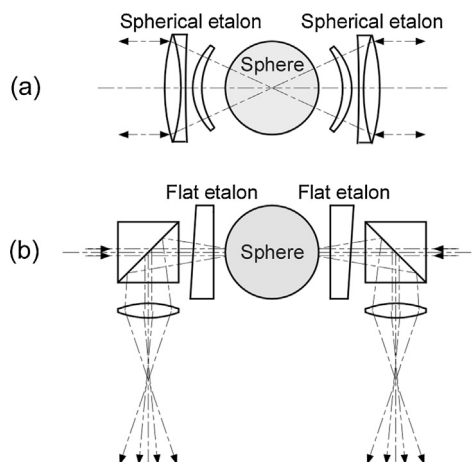


**Fig. 4.** Optical interferometers used to measure the diameter of silicon spheres. Optical configurations used at PTB (a) and at NMIJ (b) [16,17]. Adapted from <http://iopscience.iop.org/article/10.1088/0026-1394/41/2/S01/meta#metro176796fig03>. With kind permission of IOP Publishing.

effect [14]. Therefore, INRiM and PTB investigated an especially designed X-ray interferometer with a lamella with stepwise different thickness. The effect could be modeled and a refinement of the etching of the lamellas was carried out.

## 5. Manufacturing of the spheres and diameter measurements

For the determination of the volume of a silicon crystal, the spheres should be of nearly perfect shape, i.e. the deviation of the shape from a perfect sphere should be below 100 nm. In addition, to allow the correction of the phase retardation (see section 5.5), the oxide formed at the surface should consist only of SiO<sub>2</sub>. The crystal structure should be undisturbed up to the oxide layer, and the roughness of the sphere surface should be far below 1 nm. The new silicon spheres manufactured by PTB exhibit a shape deviation below 50 nm and a surface roughness below 0.2 nm [3]. No subsurface damage could be detected, and XPS measurements further confirmed that the oxide layers consist almost exclusively of SiO<sub>2</sub> [3].

### 5.1. Diameter measurements

The core volume of the Si sphere is measured by optical interferometry [3]. The sphere and the etalon are installed in a temperature-controlled vacuum chamber to eliminate the influences of the refractive index of air. As shown in Fig. 4, a few research institutes have developed interferometers to measure the sphere volume [15], in which the diameter is measured from many different directions. The volume is calculated from the measured mean diameter with high accuracy when the deviation from a perfect spherical shape is small.

Fig. 4a shows the optical configuration of the PTB interferometer with an etalon having spherical reference surfaces, which enable diameter measurements in numerous directions without rotating the sphere [16], whereas at NMIJ, an etalon with flat reference surfaces, shown in Fig. 4b, is used [17]. By rotating the sphere, the diameter topography of the entire sphere surface is available.

### 5.2. Interferometer with spherical reference plates (PTB)

In this interferometer, the measured quantities are the distances between the sphere's surface and the reference surfaces,  $d_1$  and  $d_2$ , and the length of the empty etalon  $D$ . Their fractional orders of interference are measured by phase-shifting interferometry using optical frequency tuning. The apparent diameter  $d$  of the sphere is then given by  $d = D - d_1 - d_2$ . Below the three-point support, there is a lifting and positioning mechanism for the sphere. When the mechanism is in the lifted position, the sphere can be rotated around horizontal and vertical axes.

This interferometer can measure about 10000 diameters of the sphere simultaneously in an aperture angle of 60°. About 20–50 different orientations of the sphere cover the entire surface of the sphere so that the volume is represented by some hundreds of thousands of diameters [18]. Fig. 5 shows an example of the volume measurement by using the PTB interferometer.

### 5.3. Interferometer with flat reference plates (NMIJ)

The sphere is placed in a fused quartz etalon with flat reference surfaces. A laser beam emitted from an external cavity laser diode is split into two beams that are reflected by mirrors towards the opposite sides of the etalon. The light beams reflected from the inner surface of the etalon plate and the adjacent surface of the sphere produce concentric circular

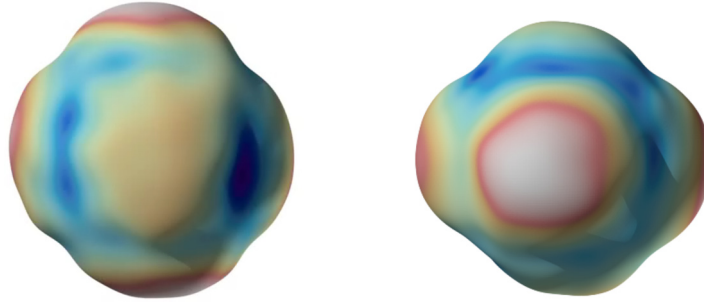


**Fig. 5.** Radius topographies of the  $^{28}\text{Si}$ -enriched spheres Si28kg02a (left) and Si28kg02b (right) manufactured from the crystal Si28-24Pr11. The maximal shape deviations from a perfect sphere are 20 nm and 28 nm, respectively.

interference fringes, which are projected onto two CCD cameras. The advantage of this configuration is that it optimizes the visibility of interference fringes [19].

The phase maps produced by phase-shifting interferometry are used to fit a linear combination of the first nine Zernike polynomials by the method of least-squares, and the fractional order of interference is calculated from the extremum of each phase map. The apparent diameter is given by  $d = L - d_1 - d_2$ . To determine the distance between the two etalon plates,  $L$ , a shutter intercepts one of the light beams. The other light beam passes through a hole in the lifting device, and the beams reflected from the two etalon plates produce fringes on a third CCD camera.

#### 5.4. Silicon sphere temperature measurement

A standard platinum resistance thermometer is calibrated at the triple point of water (0.01 °C) and the melting point of gallium (29.7646 °C) to ensure traceability to the thermometric fixed points of ITS-90 [20]. The linear thermal expansion coefficient of silicon crystal is about  $2.6 \cdot 10^{-6} \text{ K}^{-1}$  [21]. If, for example, an uncertainty of 1 mK is assumed for the temperature measurement of 1-kg silicon spheres, this results in a relative uncertainty of  $8 \cdot 10^{-9}$  in terms of volume. In the PTB interferometer, the temperature of the sphere is measured by thermocouples [22], whereas in the NMIJ interferometer, it is measured by platinum resistance thermometers [17], achieving sphere temperature measurements with standard uncertainties of 0.8 mK and 0.6 mK, respectively.

#### 5.5. Core volume

The sphere is covered by the surface layers described in section 7, which cause a phase retardation in the reflected light beam. The diameter measured by the interferometer therefore provides information only on the “apparent diameter”, which is different from the “core diameter”,  $D_{\text{core}}$ , introduced in section 2. To deduce  $D_{\text{core}}$ , the total phase retardation on the reflection from the sphere surface, which includes the influence of multiple reflections in the surface layers, should be evaluated from surface measurements given in section 7.

The surface layers (SL) consist mainly of  $\text{SiO}_2$ . In addition, a chemisorbed water layer, a physisorbed water layer, and a carbonaceous layer are present on the surface. When the reference phase is set at the top of the surface layers, a total phase retardation,  $\delta$ , on reflection at the surface layers with a total thickness,  $d_{\text{SL}}$ , is given by considering the complex refractive index of each layer. By calculating the overall amplitude reflection coefficients of the reflected light beam from the silicon sphere,  $\delta$  is derived from the procedure given in [3,17], where  $\delta$  is usually a little less than  $\pi$ , and decreases with increasing the thickness of the surface layers. The difference between the mean apparent diameter,  $D_{\text{apparent}}$ , observed by interferometry and the mean true diameter ( $D_{\text{sphere}} = D_{\text{core}} + 2d_{\text{SL}}$ ) is then given by  $\Delta d = \lambda (\delta - \pi)/(2\pi)$ , where  $\lambda$  is the wavelength of the light beam in vacuum. The mean core diameter is thus obtained as

$$D_{\text{core}} = D_{\text{apparent}} - \Delta d - 2d_{\text{SL}} \quad (11)$$

Details on the evaluation of the thickness of each surface layer are given in section 7. The core volume is finally obtained as  $V_{\text{core}} = (\pi/6)D_{\text{core}}^3$ , as discussed in section 2. The relative standard uncertainties in the core volume measurement by the two interferometers are below  $2 \cdot 10^{-8}$ , giving a consistent result in the core volume measurement [14].

The largest uncertainty source in the volume measurement is currently attributed to the wave-front aberration in the PTB interferometer and to the diffraction effect of optical wave propagation in the NMIJ interferometer. Optical simulations and experimental verifications for those influences are therefore being conducted at PTB and NMIJ to further reduce the uncertainty in the volume measurement of the silicon spheres.

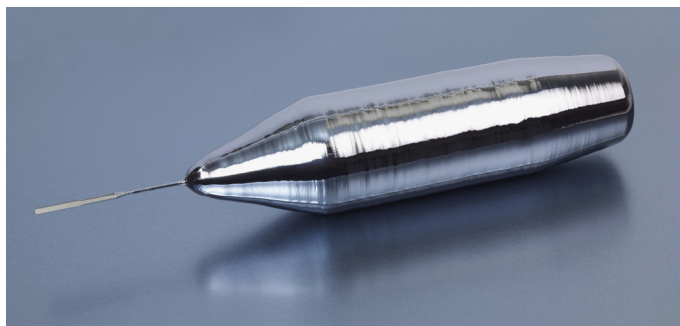


Fig. 6. The newest  $^{28}\text{Si}$  single-crystal Si28-31Pr11 (mass 5682 g, maximal diameter 101 mm).

Table 1

Isotopic enrichment of the four large Si28 single crystals.

Crystal	Enrichment in $^{28}\text{Si}$	Reference
AVO28	99.9958%	[3]
Si28-23Pr11	99.9984%	[3]
Si28-24Pr11	99.9993%	[3]
Si28-31Pr11	99.9985%	[this paper]

## 6. Isotope enrichment and measurement

To reach the highest accuracy with the XRCd method, the silicon material must be chemically extremely pure and the enrichment of the  $^{28}\text{Si}$  isotope should be higher than 99.99%. Up to now, four suitable large Si-28 crystals exist (see Fig. 6) and two more will be grown soon. Two 1-kg spheres were or will be manufactured from each crystal.

Gaseous silicon tetrafluoride  $\text{SiF}_4$  is used to enrich the  $^{28}\text{Si}$  isotope.  $\text{SiF}_4$  can be produced from natural silicon and gaseous fluorine:



Since fluorine consists of only one isotope, the  $^{28}\text{Si}$  isotope can be isotopically enriched by centrifugation of  $\text{SiF}_4$  [23]. After transforming the enriched  $\text{SiF}_4$  into silane ( $^{28}\text{SiH}_4$ ) using calcium hydride ( $\text{CaH}_2$ )



the silane is cleaned in a very sophisticated procedure by cryofiltration with subcooled boiling and rectification [23]. Eventually, the enriched silicon is deposited by pyrolytic vapor deposition on a slim, electrically heated Si-28 rod. The produced polycrystalline silicon rod is purified by the float zone technique, first in vacuum to remove oxygen and later in argon. Nitrogen is added in the final growth of the single crystal in order to prevent the agglomeration of vacancies. The isotopic enrichment of the existing four large Si-28 crystals is listed in Table 1. All four monocrystals were grown by the Leibniz Institute for Crystal Growth (IKZ, Berlin, Germany) using polycrystalline material that was deposited at the G.G. Devyatikh Institute of Chemistry of High-Purity Substances of the Russian Academy of Sciences (IChHPS RAS, Nizhny Novgorod, Russia). The isotopic enrichment of the first (AVO28) material was performed at the Science & Technical Center ‘Centrotech’ (CT, St. Petersburg, Russia) [24], whereas the other materials were enriched at the Stock Company Production Association Electrochemical Plant (SC ‘PA ECP’, Zelenogorsk, Russia) [23].

For the realization of the mass unit with Eq. (7), the mean relative atomic mass or the amount of substance fractions of the silicon material have to be determined. If  $^{29}\text{Si}$  and  $^{30}\text{Si}$  are interpreted as a kind of contamination in the silicon material, they can be measured by the isotope dilution mass spectrometric (IDMS) method. The amount of this ‘virtual element’ (VE) consisting of only  $^{29}\text{Si}$  and  $^{30}\text{Si}$  can thus be determined with relative uncertainties below 1% [1]. Since natural silicon contains about 5% of  $^{29}\text{Si}$  and 3% of  $^{30}\text{Si}$ , this allows the mean relative atomic mass  $A_r(\text{Si})$  to be determined with an uncertainty in the order of 10 ppm. Far lower uncertainties are reached with isotopically enriched silicon.

For the IDMS method, the silicon samples are carefully cleaned and etched to remove all surface contaminations. Then the samples are weighed to determine their masses and dissolved in tetramethylammonium hydroxide (TMAH) [1]. The solutions are measured by high-resolution multi-collector inductively coupled plasma mass spectrometry (HR-MC-ICP-MS). The unknown Si-28 sample (labeled ‘x’) is mixed with a material highly enriched in the isotope  $^{30}\text{Si}$  (labeled ‘y’) yielding the so-called blend (labeled ‘bx’). The mass of the Si-28 sample,  $m_x$ , and of the Si-30 spike,  $m_{y,x}$ , used for the mixture are measured to determine the ratio  $m_{y,x}/m_x$ . For isotope dilution, only the isotope ratios  $R_2 = x(^{30}\text{Si})/x(^{29}\text{Si})$  have to be measured in the sample (x), the spike enriched in  $^{30}\text{Si}$  (y) and the blend (bx). The ratio  $R_3 = x(^{28}\text{Si})/x(^{29}\text{Si})$  is additionally measured for the spike (see Eq. (14) and Fig. 7).



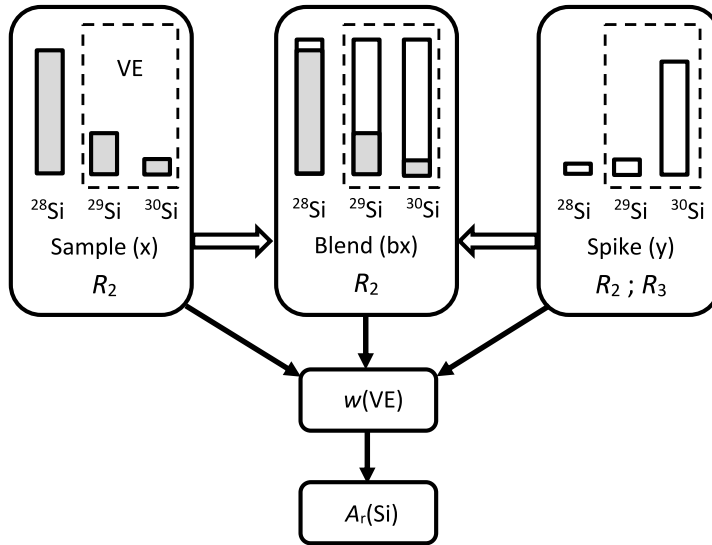


**Fig. 7.** Principle of the virtual element IDMS: The virtual element (VE) consists of the  $^{29}\text{Si}$  and  $^{30}\text{Si}$  isotopes (dashed frames). The isotope ratios  $R_2 = x(^{30}\text{Si})/x(^{29}\text{Si})$  are measured in the sample (x), blend (bx), and spike (y). The ratio  $R_3 = x(^{28}\text{Si})/x(^{29}\text{Si})$  is measured only in the spike. This yields the mass fraction  $w(\text{VE}) = w(^{29}\text{Si}) + w(^{30}\text{Si})$  and then the mean relative atomic mass  $A_r(\text{Si})$ .

**Table 2**

Thickness and mass of surface layers on the Si28kg01b sphere in vacuum measured at PTB by XRF/XPS (in brackets: standard uncertainty) [14].

Surface layer	Thickness in nm	Mass in $\mu\text{g}$
Water	0.26(12)	7.1(3.3)
Carbon	0.43(17)	12.0(4.1)
Oxide	0.96(14)	58.2(8.0)

$$A_r(\text{Si}) = \sum_{i=28}^{30} x(^i\text{Si}) A_r(^i\text{Si}) = \frac{A_r(^{28}\text{Si})}{1 + \frac{m_{\text{yx}}}{m_x} \frac{(1+R_2(x))A_r(^{28}\text{Si}) - A_r(^{29}\text{Si}) - R_2(x)A_r(^{30}\text{Si})}{R_3(y)A_r(^{28}\text{Si}) + A_r(^{29}\text{Si}) + R_2(y)A_r(^{30}\text{Si})} \frac{R_2(y) - R_2(\text{bx})}{R_2(\text{bx}) - R_2(x)}}} \quad (14)$$

All isotope ratios must be corrected for the blank concentration in the used TMAH. The mass spectrometer must be silicon-free, e.g. by using a sapphire torch.

Due to a small mass discrimination in the mass spectrometer, the measured isotope ratios have to be corrected by calibration factors which are determined with additional mixtures of  $^{28}\text{Si}$ ,  $^{29}\text{Si}$  and  $^{30}\text{Si}$ , see [1]. The lowest standard uncertainty reached up to now is about  $1 \cdot 10^{-9}$  relatively for the crystal Si28-24Pr11 [1], which has an enrichment higher than 99.999% (Table 1).

## 7. Surface characterization

Silicon samples are generally covered with 1-nm-thick layers of silicon oxides and 0.5-nm-thick layer of carbon-containing compounds, and – in vacuum – one monolayer of water (compare with Table 2). For a 1-kg silicon sphere, this results in a mass of about 100  $\mu\text{g}$ . A 1-g silicon sphere would have about 1  $\mu\text{g}$  of surface layers. Although a lot of methods for surface characterization exist, most apparatuses are neither able to accommodate a large 1 kg sphere nor to rotate the sphere automatically in order to map the whole surface.

The X-ray reflectometry (XRR) method can measure the thickness of a layer traceable to the SI meter with a standard uncertainty of 0.1 nm, but it is rather time consuming and most suitable for oxide layer larger than 5 nm, since then interference patterns occur. Therefore, the XRR method is usually only used to calibrate small reference samples for the calibration of other methods [25].

The X-ray fluorescence (XRF) spectroscopy can detect and measure most chemical elements on the surface, but has to be calibrated by suitable reference samples. It measures directly the surface density or mass per unit area, which is primarily needed for Eq. (7).

Most suitable for the thin layers on silicon samples is X-ray photoelectron spectroscopy (XPS). This method cannot only detect and measure the chemical elements on the surface, but also the chemical binding state of the elements. This allows the stoichiometric composition of the layers to be determined. Thus, it can be used to prove that the oxide layer consists of nearly perfect silicon dioxide ( $\text{SiO}_2$ ). Similarly, the chemical composition of the carbonaceous layer can be clarified by

**Table 3**

Typical concentration of point defects (impurities and vacancies) in pure silicon and the resulting mass corrections for a 1-kg sphere.

Defect	Concentration in $10^{15} \text{ cm}^{-3}$	Mass deficit in $\mu\text{g}$
Carbon	1.5	17.1
Oxygen	0.2	−2.3
Nitrogen	0.05	−0.5
Vacancy	0.3	6.0

XPS. Since the XPS signal of the silicon bulk is affected by crystal orientation [26], this signal can only be used in the measurement if it is possible to avoid low-indexed crystal orientations [27].

XPS and XRF can be combined in one apparatus [28], thus enabling a complete characterization of the surface layers in one apparatus. Nowadays, relative standard uncertainties of below 10  $\mu\text{g}$  for a 1-kg sphere are reached. Whereas the above-mentioned methods are very difficult and expensive, the spectral ellipsometry (SE) is a simple and very rapid method to fully map the oxide layer of a sphere. SE has to be calibrated, either by using plane reference samples or by using points on the sphere that have been measured with XRR [14,25].

Some more fundamental investigations were made by the gravimetric method, e.g., the amount of water on silicon in air and vacuum was measured by weighing [29].

## 8. Crystal perfection

Nowadays, large silicon crystals can be grown that are extremely pure and do not contain dislocations. Due to the sophisticated cleaning procedure (see section 6) of the Si-28 material, the enriched crystals contain even less impurities than natural silicon crystals from large-scale production. Therefore, the only important impurities are carbon and oxygen, which can be quantified by Fourier-Transform Infrared Absorption Spectroscopy (FTIR) measurements at low temperature [30]. The amount of these impurities influences the mass of the silicon spheres by only 10  $\mu\text{g}/\text{kg}$  to 30  $\mu\text{g}/\text{kg}$  (Table 3). All other impurities – if detectable at all – are nearly negligible and affect the mass of the sphere only by about 1  $\mu\text{g}$  per kg. To ensure the purity of the crystals, the following survey methods are used: the “instrumental neutron activation analysis” (INAA) by neutron activation of the atomic nucleus [31] and mass spectrometric measurements like glow discharge mass spectrometry.

The Si-28 crystals are grown in the “vacancy region”, i.e. the growth velocity is chosen large enough that the vacancies are in the majority over self-interstitials after freezing and therefore annihilate the self-interstitials. The concentration of vacancies in such crystals ranges from zero to about  $5 \cdot 10^{14} \text{ cm}^{-3}$  [32].

The point defects (i.e. impurities and vacancies) affect the lattice parameter and the density of the silicon, but these effects cancel each other and only the “mass deficit” must be considered [14]:

$$m_{\text{deficit}} = V_{\text{core}} \sum_x (m_{28} - m_x) N_x \quad (15)$$

This calculates the mass difference between a sphere having Si atoms occupying all regular sites and the real sphere. In Eq. (15),  $m_{28}$  and  $m_x$  are the masses of a  $^{28}\text{Si}$  atom and the point defect is referred to as  $x$ , respectively. For a vacancy,  $m_x = m_v = 0$ . For interstitial point defects,  $m_x$  is the sum of the masses of the defect and a  $^{28}\text{Si}$  atom.  $N_x$  is the concentration of the point defect  $x$ .

## 9. Dissemination of the mass unit

According to the new definition, and following Eq. (7), the mass of a silicon sphere can be determined only in relation to the Planck constant and by characterizing its properties, such as the lattice parameter and the molar mass of the crystal, and the volume of the sphere, corrected for its surface layers. As this procedure does not need a comparison with or a measurement against another mass standard, this silicon sphere can be used as a primary mass standard.

For the maintenance and dissemination of the realization of the mass unit, key comparisons between different primary mass standards or comparison measurements between primary masses and transfer or secondary standards have to be carried out. These comparisons are distinguished according to whether they can be performed in vacuum or in air. As for the first, buoyancy and sorption effects can be neglected and so smallest uncertainties can be reached, however, for the latter, surface and volume effects must be considered. There are mass standards of silicon, platinum–iridium, and stainless steel. Due to their density differences, they have different volumes, therefore different buoyancy, and different surface areas, i.e. different sorption of water and other compounds of the direct environment. For a precise estimate of the sorption effects between vacuum and air and for the different materials, so called sorption artefacts were manufactured [33], see Fig. 8. Typically, this is a pair of mass pieces, which are equal in mass, volume and material, especially their surface finishing, but different in their total area of surface. For example, one artefact is a cylinder of mass 1 kg, and the other is a set of, e.g., 10 slices, in sum also 1 kg, of the same material and polishing condition, but with a surface of about four times the area. If

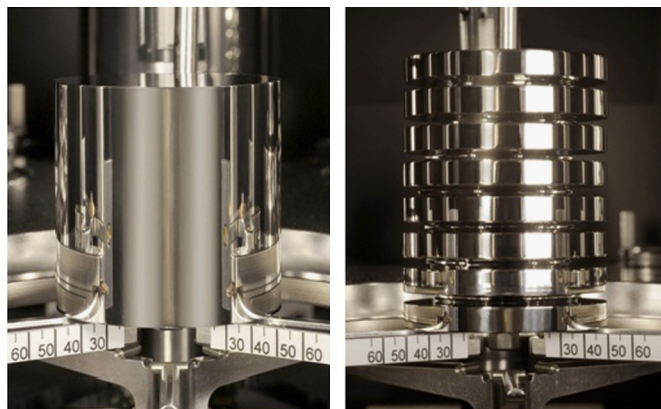


Fig. 8. Sorption artefacts made of PtIr on weighing pans.

Table 4

Foreseen uncertainty budget for the realization of the kilogram by the XRCD method.

Quantity	Relative standard uncertainty/ $10^{-9}$
Planck constant $h$	0
$h/m(^{28}\text{Si})$	<1
Lattice parameter	5
$A_r(\text{Si}) = \sum_j x(^i\text{Si})A_r(^i\text{Si})$	5
Point defects	5
Surface layer	10
Volume of the sphere	15
Total uncertainty	20

the mass of this pair is measured in air and in vacuum, then the measured differences allow the sorption to be determined in terms of surface area. With this, the standard deviations of a few micrograms can be achieved for the vacuum-to-air transfer.

## 10. Uncertainty in the XRCD method

For the final determination of the Avogadro constant by the XRCD method [14,34], a big group of institutes contributed their results, partially redundant, to ensure a small uncertainty. The relative standard uncertainty of the mean value could be given with  $1.2 \cdot 10^{-8}$ . Mainly four quantities, volume and mass of the spheres and molar mass and lattice parameter of the crystal, directly contribute to the Avogadro constant, and composition and thickness of surface layers are the largest correction quantities. Among these quantities, the volume determination of silicon spheres has the largest relative standard uncertainty, compare with Table 4. Advantageously, two institutes, NMIJ and PTB, with in general different interferometers, are able to determine the volume independently. Two  $^{28}\text{Si}$  crystals each with two silicon spheres, all slightly different in size and form, but close to 1 kilogram, were measured alternately. They showed an excellent agreement for each of the spheres of better than 0.3 nm for the mean diameter. Both institutes are working on improvements to reduce the uncertainty furthermore (compare with section 5).

The second largest contribution to the total uncertainty is the determination of the mass of the surface layers. At NMIJ and PTB, the mass and thickness of the surface layers are accurately determined using XPS and XRF. Although some assumptions on constitution and density of the surface layers must be made, and the values of thickness and mass end up with a standard uncertainty of about 10 percent, the total impact on the mass determination of the sphere is only 10  $\mu\text{g}$ .

The newer  $^{28}\text{Si}$ -enriched crystals are higher enriched and the impurity concentrations are reduced, so that the measurement uncertainties of  $A_r(\text{Si}) = M(\text{Si})/M_u$  decrease, and the point-defect concentrations are reduced.

For the lattice parameter measurement, the new and independent set-up of PTB will confirm the existing value of INRIM and will reduce the overall uncertainty.

Therefore, in the near future, a relative standard uncertainty of about 1 part in  $10^8$  will be reached as a regular realization of the redefined kilogram by XRCD. After the redefinition, every institute that owns a sphere will measure the spheres by its own set of devices. This might result in a larger uncertainty for the realization of the kilogram – e.g., see Table 4.

The results of the realizations must be checked for consistency by key comparisons organized by the Consultative Committee for Mass and Related Quantities (CCM). If the crystal parameters, such as molar mass, impurity concentrations, and lattice parameter, are already evaluated for the silicon crystal to be used for the realization, their published values can be used.

If a  $^{28}\text{Si}$ -enriched crystal is produced, and the amount-of-substance fractions  $x(^i\text{Si})$  and the lattice constant  $a$  are determined, it can be assumed that these values will not change for any samples prepared from this crystal if it is not exposed to extreme environment conditions. Therefore, it will last out the realization of the kilogram to measure the diameter and the surface layers of a sphere of that crystal. It will turn out that the XRCD method is very convenient and effective for realizing the kilogram, as the measurements of the molar mass and of the lattice parameter have not to be repeated, even if, for instance, the sphere should be re-polished. CCM expects for the realization that a relative standard uncertainty of  $2 \cdot 10^{-8}$  or a standard uncertainty of  $20 \mu\text{g}$  will not be exceeded in the realization of the kilogram.

## 11. Relative measuring methods

The absolute measurement of the main quantities of Eq. (7) with uncertainties below  $1 \cdot 10^{-8}$  is extremely difficult. Therefore, precision differential methods have been developed to check the absolute measurements and also to evaluate new crystals or spheres in comparison to absolute measurements.

Relative lattice parameter measurements were performed to investigate the homogeneity of the crystal lattice and to measure the lattice parameter difference between natural silicon and the Si-28 crystal AVO28 [35]. Additionally, the lattice parameter of the new Si-28 crystal Si28-23Pr11 was determined by comparison to the AVO28 crystal by a self-referenced lattice comparator (SRLC) at the Photon Factory of the High Energy Accelerator Research Organization (KEK) in Japan [14,36]. PTB currently sets up a new apparatus for lattice distance comparisons.

Similarly, density difference measurements by the pressure-of-flotation method (PFM) can check absolute measurements of the density  $\rho = m/V$  that have been determined by absolute mass and volume measurements. Also, the unknown density of a silicon sample can be determined by comparison to an absolutely measured sphere. The PFM can reach standard uncertainties of  $1 \cdot 10^{-8} \rho$  [22]; however, since it has a very small measuring range of about 10 ppm, a measurement of the relative density difference between natural silicon and enriched silicon of about 0.4% is not possible. For this purpose, PTB builds up a hydrostatic comparison apparatus using a magnetic suspension coupling that aims to reach relative standard uncertainties of a few  $10^{-8}$  [37]. With this “magnetic flotation” method, the density of natural silicon can be calibrated traceable to the density of a  $^{28}\text{Si}$  sphere. Thus, natural silicon spheres can be used to realize the mass unit with highest accuracy after an additional volume determination:  $m = \rho V$  and to calculate the molar mass or mean relative atomic mass  $A_r(\text{Si})$  of the natural crystal – compare Eqs. (7) and (14).

Relative measurements of the isotopic composition of enriched silicon crystals have been made by mass spectrometric comparison with potassium as an internal isotopic standard at the G.G. Devyatikh Institute of Chemistry of High-Purity Substances of the Russian Academy of Sciences (IChHPS RAS) [23]. Similarly, relative measurements by IDMS should in principle be possible.

## 12. Discussion

The new definitions of the mole and kilogram will allow the realization of these units everywhere and at any time. With the XRCD method, relative uncertainties below  $2 \cdot 10^{-8}$  can be reached if isotopically enriched silicon is used. Soon twelve 1-kg Si-28 spheres will exist for the realization of the new units. Though we still have to wait until the accurate realization of the mole by this method finds practical applications, the kilogram will soon be realized and disseminated by these silicon spheres. After the characterization of an Si-28 ingot by measuring the isotopic composition, lattice parameter and point defect concentrations, only the volume and surface layers of the silicon spheres have to be measured for each new realization of the mass unit.

A sphere with natural isotopic composition can also be used for the realization of the kilogram if its density is determined by a high-precision hydrostatic comparison to a Si-28 sphere [37]. Another possible way is the determination of the isotopic composition of natural silicon if a relative uncertainty of a few parts in  $10^5$  is enough. This is in particular valid for small masses below 1 mg where relative standard uncertainties of  $10^{-4}$  are aimed at. If the density of the natural silicon ingot is calculated from the molar mass or measured in comparison to density standards, the mass of a small sample can be determined simply by an additional volume measurement using  $m = \rho V$ .

Additionally, the mass of a secondary mass standard manufactured from silicon can be monitored by surface layer measurements (and occasional volume determinations), thus avoiding the need for re-calibrations by a primary mass standard.

The XRCD method is thus versatile not only for the realization of the kilogram at the highest accuracy level, but also for the realization of the small mass values and for the dissemination by secondary mass standards. It should be noted that all these new possibilities in measurements are realized by replacing the artefact-dependent definition of the kilogram with a fundamental constant of nature. This new concept in the revised SI is strongly expected to further create newer principles in measuring mass and related quantities.

## References

- [1] B. Güttler, O. Rienitz, A. Pramann, The Avogadro constant for the definition and realization of the mole, *Ann. Phys.* (2018) 1800292, pp. 1–17.
- [2] I.A. Robinson, S. Schlamminger, The watt or Kibble balance: a technique for implementing the new SI definition of the unit of mass, *Metrologia* 53 (2016) A46–A74.

- [3] K. Fujii, H. Bettin, P. Becker, E. Massa, O. Rienitz, A. Pramann, A. Nicolaus, N. Kuramoto, I. Busch, M. Borys, Realization of the kilogram by the XRCd method, *Metrologia* 53 (2016) A19–A45.
- [4] U. Bonse, M. Hart, An X-ray interferometer, *Appl. Phys. Lett.* 6 (1965) 155–156.
- [5] A. Leistner, G. Zosi, Polishing a 1-kg silicon sphere for a density standard, *Appl. Opt.* 26 (1987) 600–601.
- [6] P. Becker, et al., Large-scale production of highly enriched  $^{28}\text{Si}$  for the precise determination of the Avogadro constant, *Meas. Sci. Technol.* 17 (2006) 1854–1860.
- [7] O. Rienitz, A. Pramann, D. Schiel, Novel concept for the mass spectrometric determination of absolute isotopic abundances with improved measurement uncertainty: part 1 – theoretical derivation and feasibility study, *Int. J. Mass Spectrom.* 289 (2010) 47–53.
- [8] K. Fujii, E. Massa, H. Bettin, N. Kuramoto, G. Mana, Avogadro constant measurements using enriched  $^{28}\text{Si}$  monocrystals, *Metrologia* 55 (2018) L1–L4.
- [9] D.B. Newell, F. Cabiati, J. Fischer, K. Fujii, S.G. Karshenboim, H.S. Margolis, E. de Mirandes, P.J. Mohr, F. Nez, K. Pachucki, T.J. Quinn, B.N. Taylor, M. Wang, B.M. Wood, Z. Zhang, The CODATA 2017 values of  $h$ ,  $e$ ,  $k$ , and  $N_A$  for the revision of the SI, *Metrologia* 55 (2018) L13–L16.
- [10] P.J. Mohr, D.B. Newell, B.N. Taylor, E. Tiesinga, Data and analysis for the CODATA 2017 special fundamental constants adjustment, *Metrologia* 55 (2018) 125–146.
- [11] P. Cladé, F. Biraben, L. Julien, F. Nez, S. Guellati-Khélifa, Precise determination of the ratio  $h/m_u$ : a way to link microscopic mass to the new kilogram, *Metrologia* 53 (2016) A75–A82.
- [12] P.J. Mohr, D.B. Newell, B.N. Taylor, CODATA recommended values of the fundamental physical constants: 2014, *Rev. Mod. Phys.* 88 (2016) 035009, pp. 1–73.
- [13] R.H. Parker, C. Yu, W. Zhong, B. Estey, H. Müller, Measurement of the fine-structure constant as a test of the Standard Model, *Science* 360 (2018) 191–195.
- [14] G. Bartl, et al., A new  $^{28}\text{Si}$  single crystal: counting the atoms for the new kilogram definition, *Metrologia* 54 (2017) 693–715.
- [15] N. Kuramoto, K. Fujii, A. Nicolaus, G. Bartl, M. Gray, P. Manson, W. Giardini, Diameter comparison of a silicon sphere for the international Avogadro coordination project, *IEEE Trans. Instrum. Meas.* 60 (2011) 2615–2620.
- [16] R.A. Nicolaus, K. Fujii, Primary calibration of the volume of silicon spheres, *Meas. Sci. Technol.* 17 (2006) 2527–2539.
- [17] N. Kuramoto, K. Fujii, K. Yamazawa, Volume measurement of  $^{28}\text{Si}$  spheres using an interferometer with a flat etalon to determine the Avogadro constant, *Metrologia* 48 (2011) S83–S95.
- [18] G. Bartl, H. Bettin, M. Krystek, T. Mai, A. Nicolaus, A. Peter, Volume determination of the Avogadro spheres of highly enriched  $^{28}\text{Si}$  with a spherical Fizeau interferometer, *Metrologia* 48 (2011) S96–S103.
- [19] K. Fujii, R. Masui, S. Seino, Volume determination of fused quartz spheres, *Metrologia* 27 (1990) 25–31.
- [20] H. Preston-Thomas, The international temperature scale of 1990 (ITS-90), *Metrologia* 27 (1990) 3–10.
- [21] G. Bartl, A. Nicolaus, E. Kessler, R. Schödel, P. Becker, The coefficient of thermal expansion of highly enriched  $^{28}\text{Si}$ , *Metrologia* 46 (2009) 416–422.
- [22] B. Andreas, et al., Counting the atoms in a  $^{28}\text{Si}$  crystal for a new kilogram definition, *Metrologia* 48 (2011) S1–S13.
- [23] N.V. Abrosimov, et al., A new generation of 99.999% enriched  $^{28}\text{Si}$  single crystals for the determination of Avogadro's constant, *Metrologia* 54 (2017) 599–609.
- [24] P. Becker, et al., Large-scale production of highly enriched  $^{28}\text{Si}$  for the precise determination of the Avogadro constant, *Meas. Sci. Technol.* 17 (2006) 1854–1860.
- [25] I. Busch, Y. Azuma, H. Bettin, L. Cibik, P. Fuchs, K. Fujii, M. Krumrey, U. Kuetgens, N. Kuramoto, S. Mizushima, Surface layer determination for the Si spheres of the Avogadro project, *Metrologia* 48 (2011) S62–S82.
- [26] M.P. Seah, et al., Critical review of the current status of thickness measurements for ultra thin  $\text{SiO}_2$  on Si – part v: results of a CQM pilot study, *Surf. Interface Anal.* 36 (2004) 1269–1303.
- [27] L. Zhang, N. Kuramoto, Y. Azuma, A. Kurokawa, K. Fujii, Thickness measurements of oxide and carbonaceous layer on a  $^{28}\text{Si}$  sphere by XPS, *IEEE Trans. Instrum. Meas.* 66 (2017) 1297–1303.
- [28] M. Müller, B. Beckhoff, E. Beyer, E. Darlatt, R. Fliegau, G. Ulm, M. Kolbe, Quantitative surface characterization of silicon spheres by combined XRF and XPS analysis for the determination of the Avogadro constant, *Metrologia* 54 (2017) 653–662.
- [29] S. Mizushima, Determination of the amount of gas adsorption on  $\text{SiO}_2/\text{Si}(100)$  surfaces to realize precise mass measurement, *Metrologia* 41 (2004) 137–144.
- [30] S. Zakel, S. Wundrack, H. Niemann, O. Rienitz, D. Schiel, Infrared spectrometric measurements of impurities in highly enriched ‘Si28’, *Metrologia* 48 (2011) S14–S19.
- [31] G. D’Agostino, M.D. Luzio, G. Mana, M. Oddone, J.W. Bennett, A. Stopic, Purity of  $^{28}\text{Si}$ -enriched silicon material used for the determination of the Avogadro constant, *Anal. Chem.* 88 (2016) 6881–6888.
- [32] V.V. Voronkov, R. Falster, Intrinsic point defects in silicon crystal growth, *Solid State Phenom.* 178–179 (2011) 3–14.
- [33] S. Davidson, J. Berry, P. Abbott, K. Marti, R. Green, A. Malengo, L. Nielsen, Air-vacuum transfer; establishing traceability to the new kilogram, *Metrologia* 53 (2016) A95–A113.
- [34] Y. Azuma, et al., Improved measurement results for the Avogadro constant using a  $^{28}\text{Si}$ -enriched crystal, *Metrologia* 52 (2015) 360–375.
- [35] E. Massa, G. Mana, E. Ferroglio, E.G. Kessler, D. Schiel, S. Zakel, The lattice parameter of the  $^{28}\text{Si}$  spheres in the determination of the Avogadro constant, *Metrologia* 48 (2011) S44–S49.
- [36] A. Waseda, H. Fujimoto, X.W. Zhang, N. Kuramoto, K. Fujii, Uniformity evaluation of lattice spacing of  $^{28}\text{Si}$  single crystals, *IEEE Trans. Instrum. Meas.* 66 (2017) 1304–1308.
- [37] R. Wegge, H. Bettin, Development of a specialized hydrostatic comparator for the accurate density determination of natural silicon spheres: a novel method for a primary realization of the unit kilogram, in: *Proc. Conference on Precision Electromagnetic Measurements 2018 (CPEM 2018)*, Paris, France, 8–13 July, Digest, 2018, pp. 627–628.